

UC Merced

UC Merced Previously Published Works

Title

Compound Extremes Drive the Western Oregon Wildfires of September 2020

Permalink

<https://escholarship.org/uc/item/8k03m5mp>

Journal

Geophysical Research Letters, 48(8)

ISSN

0094-8276

Authors

Abatzoglou, John T
Rupp, David E
O'Neill, Larry W
[et al.](#)

Publication Date

2021-04-28

DOI

10.1029/2021gl092520

Peer reviewed

Compound extremes drive the western Oregon wildfires of September 2020

John T. Abatzoglou^{1*}, David E. Rupp², Larry W. O’Neill², Mojtaba Sadegh³

¹Management of Complex Systems Department, University of California, Merced, CA, USA;
²Oregon Climate Change Research Institute, College of Earth, Ocean, and Atmospheric Sciences,
Oregon State University, Corvallis, OR, USA; ³Department of Civil Engineering, Boise State
University, Boise, ID, USA; ⁴Oregon Climate Service, College of Earth, Ocean, and Atmospheric
Sciences, Oregon State University, Corvallis, OR, USA

* corresponding author

jabatzoglou@ucmerced.edu

orcid.org/0000-0001-7599-9750

Revised for Geophysical Research Letters

1 March 2021

Key Points

- Approximately 11% of the Oregon Cascades burned during 7-9 September 2020 coincident with strong offshore downslope winds.
- Unprecedented compound extremes involving fuel aridity and fire meteorology facilitated the extent and spread of fires.
- Very large fires in western Oregon since 1900 have generally occurred during east wind events towards the end of anomalously warm-dry summers.

29 **Abstract**

30
31 Several very large high-impact fires burned nearly 4,000 km² of mesic forests in western Oregon
32 during 7-9 September 2020. While infrequent, very large high-severity fires have occurred
33 historically in western Oregon, the extreme nature of this event warrants analyses of climate and
34 meteorological drivers. A strong blocking pattern led to an intrusion of dry air and strong
35 downslope east winds in the Oregon Cascades following a warm-dry 60-day period that
36 promoted widespread fuel flammability. Viewed independently, both the downslope east winds
37 and fuel dryness were extreme, but not unprecedented. However, the concurrence of these
38 drivers resulted in compound extremes and impacts unmatched in the observational record. We
39 additionally find that most large wildfires in western Oregon since 1900 have similarly coincided
40 with warm-dry summers during at least moderate east wind events. These results reinforce the
41 importance of incorporating a multivariate lens for compound extremes in assessing wildfire
42 hazard risk.

43

44

45 **Plain Language Summary:**

46 Several very large fires in western Oregon spread rapidly during an unusually strong offshore
47 wind event that commenced on Labor Day in 2020. The Labor Day fires burned more area of the
48 Oregon Cascades than had burned in the previous 36 years combined and very likely exceeded
49 the area burned in any single year for at least the past 120 years. The fires damaged over 4,000
50 structures, led to several fatalities, placed over 10% of the state's residents under some level of
51 evacuation advisory, and contributed to the hazardous air quality across the Northwestern US. A
52 compound set of weather-related factors leading up to and during the fires facilitated these
53 extreme fires. Unusually warm conditions with limited precipitation in the 60-days leading up to
54 the fires allowed for fuels to become particularly dry and combustible by early September.
55 Downslope offshore winds materialized during 7-9 September 2020 across the Oregon Cascades
56 bringing exceptionally strong winds and dry air that drove rapid rates of fire spread. While
57 neither of these individual factors were unprecedented, the concurrence of these drivers
58 created conditions unmatched in the observational record.

59 1. Introduction

60

61 On Labor Day, 7 September 2020, exceptionally strong east-to-northeast winds developed from
62 Washington state progressing southward in the following days driving extreme fire activity in
63 Washington, Oregon, and California. In western Oregon, the winds fanned several existing small,
64 smoldering wildfires ignited by lightning several weeks prior, and contributed to numerous new
65 human-caused fires that spread rapidly. Dry katabatic winds drove fire spread towards populated
66 areas in the ensuing three days, hindering fire suppression efforts already strained by the
67 numerous concurrent large fires burning across much of the western US during a fire season of
68 record high atmospheric aridity in much of the region (Higuera & Abatzoglou, 2020). About
69 40,000 people in Oregon were forced to evacuate their homes, and roughly 500,000 were under
70 some level of evacuation alert during the event. In total, 393,315 hectares burned across 20
71 fires, all but a few in the Cascades of western Oregon (Fig. 1; SI Text). Moreover, over 11% of the
72 Oregon Cascades ecoregion burned in 2020, exceeding the cumulative burned area in the
73 previous 36 years (Fig. 1; SI text) and very likely exceeding annual burned area in western Oregon
74 since at least 1900. The direct cost of the series of fires was estimated at \$1.15B USD, which
75 includes the destruction of over 4,000 homes (State of Oregon, 2021).

76

77 Sustained strong winds are a major contributor to rapid rates of fire spread, particularly in the
78 presence of dry fuels (Rothermel, 1972). Of particular concern are downslope mountain winds
79 that induce adiabatic warming and entrainment of drier air leeward of mountain barriers. Such
80 winds are a well-recognized critical fire weather pattern in various parts of the globe (Nauslar et
81 al., 2018; Sharples et al., 2010). Offshore downslope winds are a catalyst for large autumn
82 wildfires in California due to the co-occurrence of offshore winds that increase throughout the
83 autumn with dry fuels prior to the arrival of winter precipitation (Guzman-Morales et al., 2016;
84 Kolden & Abatzoglou, 2018). While downslope offshore wind events west of the Cascade Range
85 in the Pacific Northwest are less frequent than counterparts in California (Abatzoglou et al.,
86 2020), significant east wind events have been implicated in major historic fires in western
87 Oregon and Washington (Beals, 1914; Dague, 1930; Cramer, 1957). The earlier arrival of cool-

88 season precipitation and higher fuel moisture in forests along the western flank of the Oregon
89 Cascades compared to California in late summer limit the co-occurrence of extreme fire weather
90 conditions with critically dry fuels.

91
92 Traditional univariate hazard assessment approaches for evaluating extreme events such as fire
93 conditioned by interacting drivers, may be ill-posed (Seneviratne et al., 2012); rather,
94 multivariate approaches that incorporate the geographic synchrony, concurrence, and
95 succession of extremes are needed to adequately characterize hazards (Sadegh et al., 2018).
96 Compound drivers have been long implicated in wildfire, including in the mesic forests of the
97 Pacific Northwest where infrequent large high-severity fires resulted from warm-dry summers
98 that enable fuel receptiveness and high winds that drive fire spread (Agee, 1996) – yet a
99 systematic analysis of compound climate and weather factors in very large fires in western
100 Oregon is lacking. Conceptual models of fire regimes consider the co-occurrence of biomass
101 abundance, availability to burn, ignitions, and weather (Bradstock, 2010) and large wildfire
102 events and seasons have been linked to compound drivers. For example, compound humidity
103 and wind speed extremes are inherent features of many critical fire weather patterns (Crimmins,
104 2006), while the combination of critically dry fuels imparted by antecedent conditions combined
105 with fire weather extremes have been connected with large fires and large fire seasons (e.g.,
106 Khorshidi et al., 2020; Williams et al., 2019). This study builds on previous efforts by applying
107 different approaches for compound extremes that supported the growth of arguably the most
108 exceptional fire outbreak in the Oregon Cascades in over a century.

109
110 In this paper we analyze the meteorological factors responsible for fire spread and antecedent
111 climate factors that enabled fuel aridity of the wind-driven fires in the western Oregon Cascades
112 whose explosive growth commenced on Labor Day 2020, hereafter referred to as the Labor Day
113 fires. We first examine the synoptic and mesoscale meteorological conditions during the Labor
114 Day fires and the rarity of individual meteorological and fuel aridity factors. We additionally use
115 different approaches for quantifying the rarity of this event through the lens of compound
116 extremes that combine fuel dryness and fire meteorology. Lastly, we systematically compare the

117 compound climate and meteorological conditions during the Labor Day fires to other very large
118 wildfire events in western Oregon since 1900.

119

120 **2. Data and Methods**

121

122 Meteorological and climatological data were obtained from several sources to address our
123 research questions. First, we acquired hourly surface observations for operational automated
124 surface observation stations (ASOS) and remote automated weather stations (RAWS) across
125 Oregon from MesoWest (Horel et al., 2002) to examine patterns of near-surface wind and vapor
126 pressure deficit (VPD) during the event. Secondly, OZ wind speed and relative humidity
127 observations at 1000hPa from version 2 of the Integrated Global Radiosonde Archive (Durre et
128 al., 2006) for Salem, Oregon for the 64-year period 1957-2020 were used to contextualize
129 meteorological conditions during the event against the longer-term data record. Third, daily
130 1/24th degree gridded meteorological data were acquired from gridMET (Abatzoglou, 2013) and
131 used to calculate two fire danger indices from the US Fire Danger Rating System (Cohen &
132 Deeming, 1985): Energy Release Component (ERC) and Burning Index (BI) for a commonly used
133 fuel model (dense conifer) for 1979-2020. These data were used to contextualize fire danger
134 during the event related to the past 42-years. Fourth, reanalysis products from the 20th Century
135 Reanalysis v3 (Compo et al., 2011) during 1900-1947, NCEP-NCAR during 1948-present, and
136 ERA5 (Hersbach et al., 2020) were used to examine mid-to-lower tropospheric synoptic
137 conditions during the event, as well as to provide context relative to the longer-term record.
138 Finally, gridded 1/24th degree monthly total precipitation and monthly mean daily maximum
139 temperature for the period 1895 – 2020 were obtained from PRISM (Daly et al., 2008) for
140 comparison of antecedent climate conditions during previous large fire events.

141

142 We use 700hPa and 850hPa zonal wind velocity from reanalysis data as a simple and transparent
143 indicator of cross-barrier downslope winds for the primarily north-south oriented Cascades
144 rather than the more refined diagnostic approaches for downslope winds developed previously
145 (Abatzoglou et al., 2020; Guzman-Morales et al., 2016). This was done by tabulating the

146 maximum easterly wind velocity in the lower troposphere 700hPa or 850hPa) near or just above
147 the crest of the Oregon Cascades at 6-hr intervals at two points: one in the Oregon Cascades at
148 45°N, 122.5°W, and the other in southwestern Oregon at 42.5°N, 122.5°W.

149

150 We accompany meteorological diagnostics with two fire danger indices – ERC and BI. ERC is
151 proxy for fuel dryness and potential energy release at the front of a fire that is a function of
152 antecedent temperature, precipitation, and humidity from previous several weeks and is
153 independent of wind speed. ERC has been shown to influence large fire probability and
154 interannual variability in regional area burned (Abatzoglou & Kolden, 2013; Barbero et al., 2014).
155 BI combines ERC and potential rate of fire spread (chiefly a function of wind speed and fuel
156 moisture) into a metric that is a proxy for flame length and fireline intensity. We examined
157 statistics of BI as it provides a natural single metric of compound extremes of fuel moisture,
158 atmospheric humidity, and wind speed that are of particular relevance for wind-driven fires.

159

160 We complement the assessment of compound extremes using rank/order statistics of
161 interrelated drivers that allow for a more flexible treatment of the resultant hazard than
162 functional equations built into a single index like BI. Two combinations were examined: (i) the
163 joint distribution of OZ relative humidity and wind speed at 1000hPa from Salem, Oregon
164 radiosonde observations during 1957-2020; (ii) the joint distribution of ERC averaged for the
165 Oregon Cascades ecoregion and lower-tropospheric easterly wind speed from reanalysis during
166 1979-2020. The former captures purely meteorological conditions, while the latter captures
167 antecedent climate and meteorological conditions. Order/rank statistics have 1:1 accordance
168 with probabilistic hazard assessment scenarios (Salvadori et al., 2016). While univariate
169 order/rank statistics correspond directly to probability $P(X < x)$, multivariate order/rank statistics
170 can take on several definitions. Herein we follow previous studies that have used a bivariate case
171 that corresponds to $P(X > x \text{ AND } Y > y)$. In this case, pairs are ranked as: $Z_i = [X_i, Y_i]$ dominates $Z_j =$
172 $[X_j, Y_j]$, if X_i dominates X_j AND Y_i dominates Y_j (AghaKouchak et al., 2014; Alizadeh et al., 2020).

173

174 Lastly, we compiled a list of very large western Oregon wildfire events ($\geq 35,000\text{ha}$) since 1900
175 (Table S1). We additionally included the 2017 Eagle Creek fire (19,761ha) because it was the
176 most recent large fire in the Oregon Cascades prior to 2020. Climate summaries for August, July-
177 August, and June-August temperature and precipitation were aggregated from the counties in
178 which each of large wildfire events occurred (Table S2). These periods were chosen because
179 most of the very large fires ignited in August and/or September. For each fire event, we
180 tabulated the maximum 6-hr easterly wind during the estimated duration of the fire at 700hPa
181 or 850hPa from 20th Century Reanalysis and NCEP-NCAR for events prior to 1948 and those since
182 1948, respectively. We note there is some uncertainty about the extent of the earliest fires and
183 fire duration, as well as potential large fire events in the first-half of the 20th century that remain
184 poorly documented. The Labor Day fires of 2020 were contextualized with other very large fires
185 within the trivariate space of antecedent temperature, antecedent precipitation, and concurrent
186 easterly wind.

187

188 **3. Results and Discussion**

189

190 Critical fire weather conditions developed from eastern Washington state southward into
191 western Oregon and northern California during 7-8 September 2020 resulting from an amplified
192 wave across the Pacific-North American sector. An omega block off the coast of British Columbia
193 and cut off low pressure near the US four corners facilitated northeasterly flow and an intrusion
194 of exceptionally dry air throughout much of the northwestern US (Fig. 2a). The onset of strong
195 east-to-northeast (ENE) winds advanced from the northern portion of the Oregon Cascades
196 during the afternoon of the 7th through southwestern Oregon into the morning of the 8th. Strong
197 ENE cross-barrier lower-tropospheric winds developed across the Oregon Cascades exhibiting a
198 classical signature of downslope winds and mountain lee wave evident by the wave pattern in
199 ERA5 pressure vertical velocity fields and downward transport of strong easterly winds and dry
200 air with relative humidities less than 10% in the lee of the Cascades (Fig. 2a,b; Fig. S1). ERA5
201 precipitable water values were less than 10mm over all of Oregon and upstream over much of
202 the U.S. west (Fig. 2a) on the afternoon of 7 Sep. The mesoscale manifestation of this pattern at

203 20 LST on 7 September 2020 shows widespread elevated surface vapor pressure deficit (VPD)
204 west of the Cascades and substantial heterogeneity in 10-m wind speeds imparted by
205 topographic station siting (Figure 2c). The strongest low-level winds were primarily constrained
206 to the evening of 7 and 8 Sep. Elevated VPD was seen for much of western Oregon for a
207 sustained 2.5 day period starting the afternoon of the 7th and with little nocturnal recovery (Fig.
208 2d).

209
210 Several individual meteorological elements of this event qualify as extremes. Observations of
211 1000hPa relative humidity and wind speed from the Salem sounding at 0Z 9 September (17 LST 8
212 September) were the 4th lowest and 7th highest values, respectively, for July-September in the
213 64-year period of record (Fig. 3a). Importantly, extreme low RH conditions co-occurred with
214 extreme high winds yielding the most extreme combination of dry-windy conditions for any July-
215 September day during 1957-2020 when viewed through the bivariate lens (Fig. 3a). Using the
216 NCEP-NCAR reanalysis record from 1948-2020 and our diagnostic of offshore downslope winds,
217 we find that 8 September 2020 had the second strongest easterly winds at 700hPa or 850hPa for
218 any July-September day (Fig. S2).

219
220 Fire danger indices of ERC and BI remained near their 1981-2010 average values for much of July
221 and early August across western Oregon (Fig. 4c-d). However, for much of August and first week
222 of September, unusually warm temperatures, elevated VPD, and negligible precipitation
223 facilitated escalating fuel dryness and well above normal ERC in parts of western Oregon by early
224 September (Fig. 4a,c). On 8 Sep, both ERC and 700/850hPa easterly wind speeds exceeded their
225 respective 99th percentile values for July-September (Fig. 3b). Similar to the meteorological
226 drivers, the co-occurrence of extremely dry fuels and strong east winds resulted in a compound
227 extreme unprecedented in the 42-year period of record, although none of the individual drivers
228 were the most extreme. Complementary to rank/order statistics, we find widespread record BI
229 across much of western Oregon on 8 September 2020 (Fig. 4b) with three of ten highest days of
230 BI for the Oregon Cascades occurring during 7-9 September 2020 (Fig. 4d). Hence, both
231 approaches for quantifying compound extremes as a product of fuel dryness and potential rate

232 of fire spread highlight conditions during the Labor Day fires as the most extreme in the
233 observational record.

234

235 The majority (ten of thirteen) of very large fire events in western Oregon since 1900 were
236 associated with a July-August that had below-median precipitation and above-median maximum
237 temperatures (Fig. 5; Fig S3-S4). Qualitatively similar results were found using June-August and
238 August temperature and precipitation data, although with somewhat weaker results for
239 precipitation (Fig. S5). More recently, all seven very large fire events since 1987 had July-August
240 precipitation at or below the 17th percentile and maximum temperature above the 70th
241 percentile. Notably, July-August 2020 was neither the driest nor the warmest per these metrics.

242

243 All thirteen very large fires were associated with a period of easterly lower-tropospheric wind
244 during the fire event (Fig. 5; see also Fig. S6). The synoptic configuration corresponding to the
245 days during each large fire event with the strongest easterly lower tropospheric flows showed
246 similarity among previous events to the Labor Day fires (Fig. S6) featuring a pronounced ridge off
247 the coast, weak thermal trough along the Oregon coast, and northeastward gradient in mean sea
248 level pressure across the region. No other very large fire had an easterly wind as strong as the
249 2020 Labor Day fires, nor were they associated with a 500-hPa level ridge and northeastward
250 sea-level pressure gradient as strong. We note that potential inhomogeneities in reanalyses
251 products inhibited a robust comparison with fields such as wind velocity (Wohland et al., 2019;
252 Fig. S7). Notably, the 1902 Columbia fire had the 2nd strongest easterly wind, yet the fire stands
253 out by having neither a dry nor a warm July-August lead-up period (Fig. 5), suggesting that it was
254 more strongly a product of immediate meteorological conditions (Beals, 1914; Plummer, 1912).
255 Previous studies have highlighted non-climatic factors as contributors to large fires in the first
256 half of the 20th century, primarily logging practices that increase dead fuel loading that help
257 facilitate flammability in the absence of anomalously warm and dry summers (Dague, 1934;
258 Kallander, 1953).

259

260 **4. Conclusions**

261
262 A series of factors contributed to the extent of fire impacts during the 2020 Labor Day fires in
263 western Oregon that burned approximately 11% of the Oregon Cascades. A sequence of climate
264 and weather factors enabled and drove rapid rates of fire spread following conceptual models of
265 fire activity (Bradstock, 2010). Moreover, while individual factors such as humidity, wind speed,
266 and fuel dryness were extreme, neither individually ranked as the most extreme on record. In
267 contrast, compound extremes of fuel dryness and low-level wind speed, as well as wind speed
268 and relative humidity, yielded conditions that were unprecedented in the contemporary data
269 record. The extent of burned area across mesic forests of western Oregon during the 2020 Labor
270 Day fires has no contemporary local analog. Very large fires (> 200,000 ha) were documented in
271 western Oregon in the 19th century coinciding with European colonization (Morris, 1934),
272 although uncertainty of the location, timing, and contributing factors limit a more detailed
273 comparison. The 2020 Labor Day fires do bear some resemblance to extremely large autumn
274 wind-driven fires in California in terms of rapid rates of fire spread and materialization of
275 compound extremes driven by offshore downslope winds at the end of the dry season when fuel
276 moisture is critically low (Nauslar et al., 2018). Non-climatic contributions to these fires imparted
277 by biomass accumulation and land management practices (Reilly et al., 2017) also likely factored
278 into this severity of fire impacts, although we do not speculate on their specific influences.

279
280 Very large fires with rapid rates of spread and extreme fire behavior are gaining attention as
281 environmental phenomena that impact society and Earth system processes (Bowman et al.,
282 2009; Khaykin et al., 2020). While the details of the meteorological, fuels, and topographic
283 drivers of such extreme fires and their impacts vary (Tedim et al., 2018), requisite conditions of
284 flammable contiguous fuels imparted by fuel drying enable extreme fires while meteorological
285 conditions including strong winds or convection often drive rapid rates of fire spread (Bowman
286 et al., 2017; Rothermel, 1991). Our findings of the Oregon 2020 Labor Day fires complement
287 previous studies on compound drivers for autumn wind-driven fires in California (Khorshidi et al.,
288 2020; Williams et al., 2019) and the development of fire early-warning systems (Jolly et al., 2019)
289 while showing the potential use of the approach for individual fire events. Moreover, the

290 approach used herein to quantify this extreme wind-driven fire events through the lens of
291 compound extremes may have value in other regions with shared biophysical and human
292 constraints on fire activity.

293
294 While unprecedented in the modern record, extreme events of this nature with widespread impact
295 evoke questions on causality – namely the extent to which human-caused climate change
296 contributed to the strength or probability of the event, as well as such events will become
297 increasingly probable in the coming decades. A formal attribution exercise is beyond the scope
298 of this analysis, yet studies suggest that climate change has contributed to increased fuel aridity
299 and longer fire seasons (Abatzoglou & Williams, 2016) and the probability of compound hot-dry
300 extremes (Alizadeh et al., 2020) and climate projections suggest continued warming with slight
301 decreases in summer precipitation in the Pacific Northwest (Rupp et al. 2017) over the 21st
302 century. By contrast, offshore winds such as Santa Ana winds in southern California may become
303 less frequent as a result of asymmetric continental warming with anthropogenic forcing
304 (Guzman-Morales & Gershunov, 2019; Hughes et al., 2011). However, few studies have formally
305 evaluated these two contrasting drivers in a compound extremes framework (Goss et al., 2020).
306 Projected changes in the confluence of extreme fire weather patterns and fuel dryness will be
307 critical for resolving future fire related hazards for mesic forests in western Oregon and
308 Washington state.

309
310

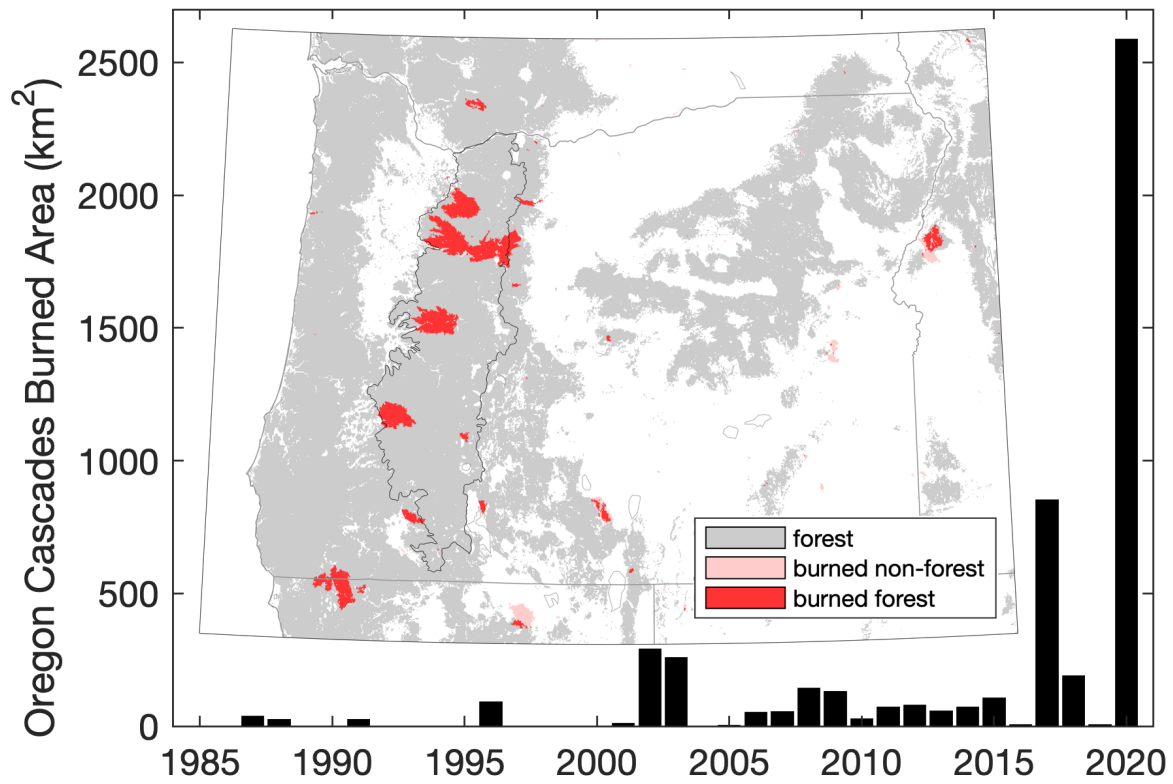
311 **Acknowledgements**

312 JTA was supported by the NSF under award OAI-2019762 and NOAA awards NA15OAR4310145
313 and NA20OAR4310478. DER was supported by the NSF under award GEO 1740082. LWO was
314 supported by the state of Oregon through the Oregon Climate Services.

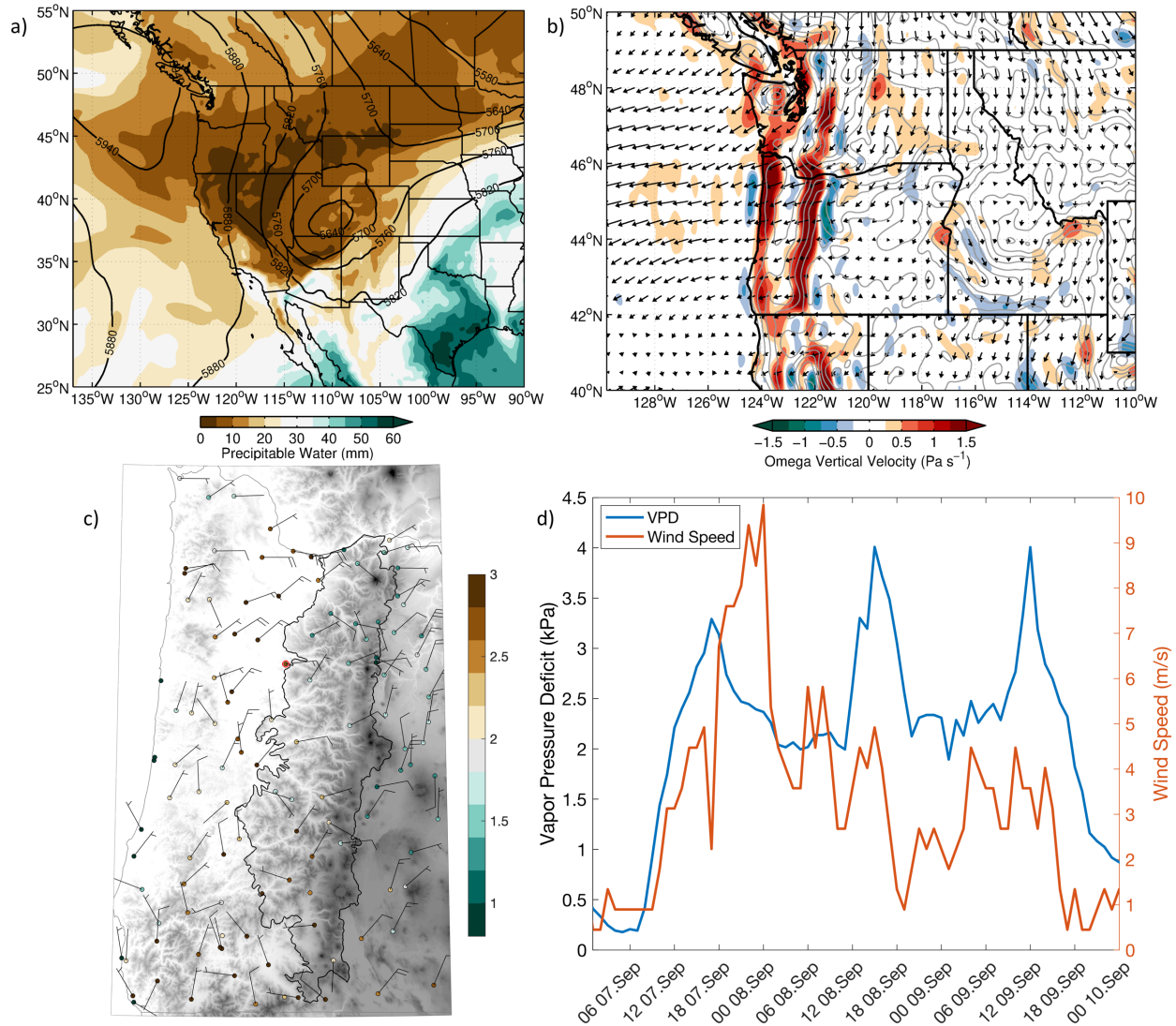
315

316 **Data availability statement:** Datasets used herein were acquired from the following public data
317 repositories: (1) ERA5: <https://cds.climate.copernicus.eu/>; (2) NCEP-NCAR reanalysis:
318 <https://psl.noaa.gov/data/gridded/data.ncep.reanalysis.html>; (3) 20th Century Reanalysis v3:
319 https://psl.noaa.gov/data/gridded/data.20thC_ReanV3.html; (4) gridMET:
320 http://thredds.northwestknowledge.net:8080/thredds/reacch_climate_MET_catalog.html; (5)
321 ASOS and RAWS station data: <https://mesowest.utah.edu/>; (6) PRISM data:
322 <https://prism.oregonstate.edu/>

323

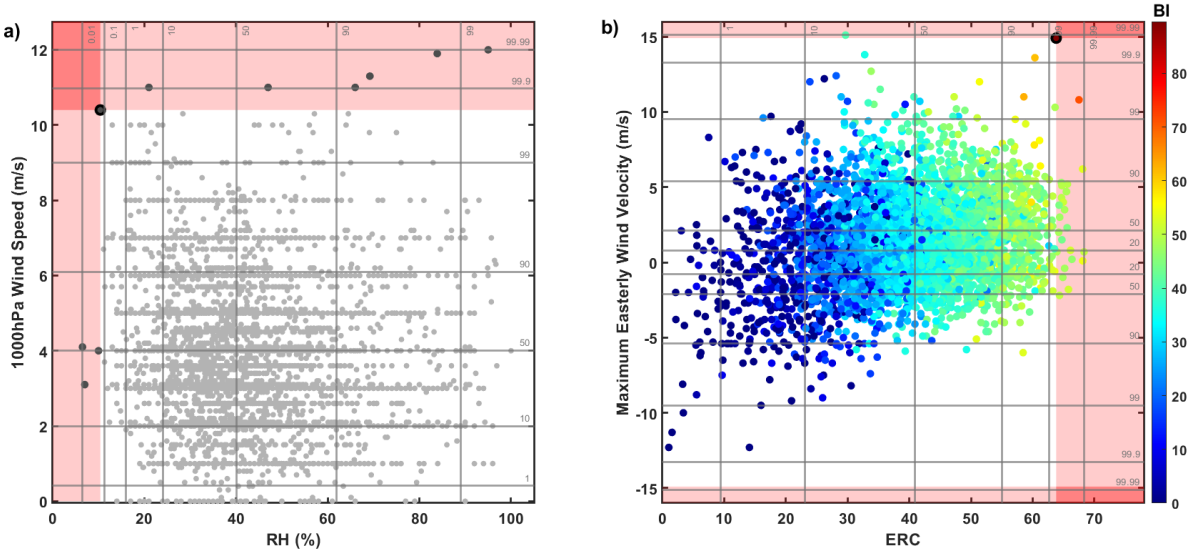


324
 325 **Figure 1:** Time series of annual burned area for the portion of the Cascades ecoregion in the
 326 state of Oregon for 1984-2020 (black polygon in inset map). Inset map shows perimeters of fires
 327 in 2020, including much of the forested burned area in western Oregon that burned during the
 328 7-9 September period.
 329



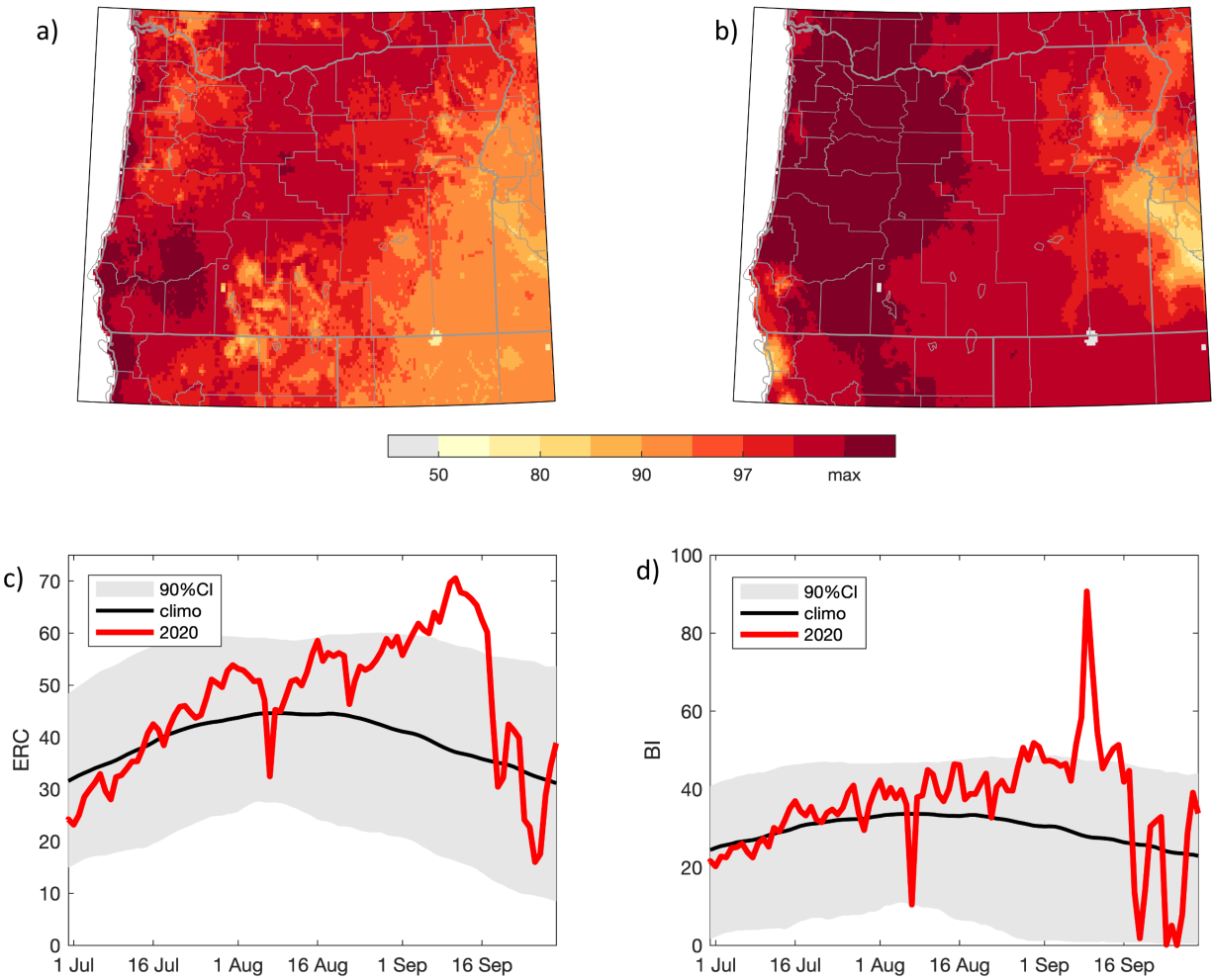
330
 331 **Figure 2:** (a) Precipitable water (shading) and 500hPa geopotential heights (contours, m), and (b)
 332 850hPa winds (vectors) and pressure vertical velocity (shading) at 0Z on 8 September 2020 (17
 333 LST on 7 Sep). In panel b, Grey contours show elevation, and red hues show downward motion
 334 while blue hues show upward motion. (c) Surface-based observations of wind speed (knots) and
 335 vapor pressure deficit (VPD, colors) at 20 LST on 7 September 2020. Grey shading in panel c
 336 depicts topography and black contour shows the Oregon Cascades ecoregion. (d) Time series of
 337 hourly wind speed and VPD from the Jordan RAWS station (red circle in panel c) during 7-9 Sep.

338
 339
 340

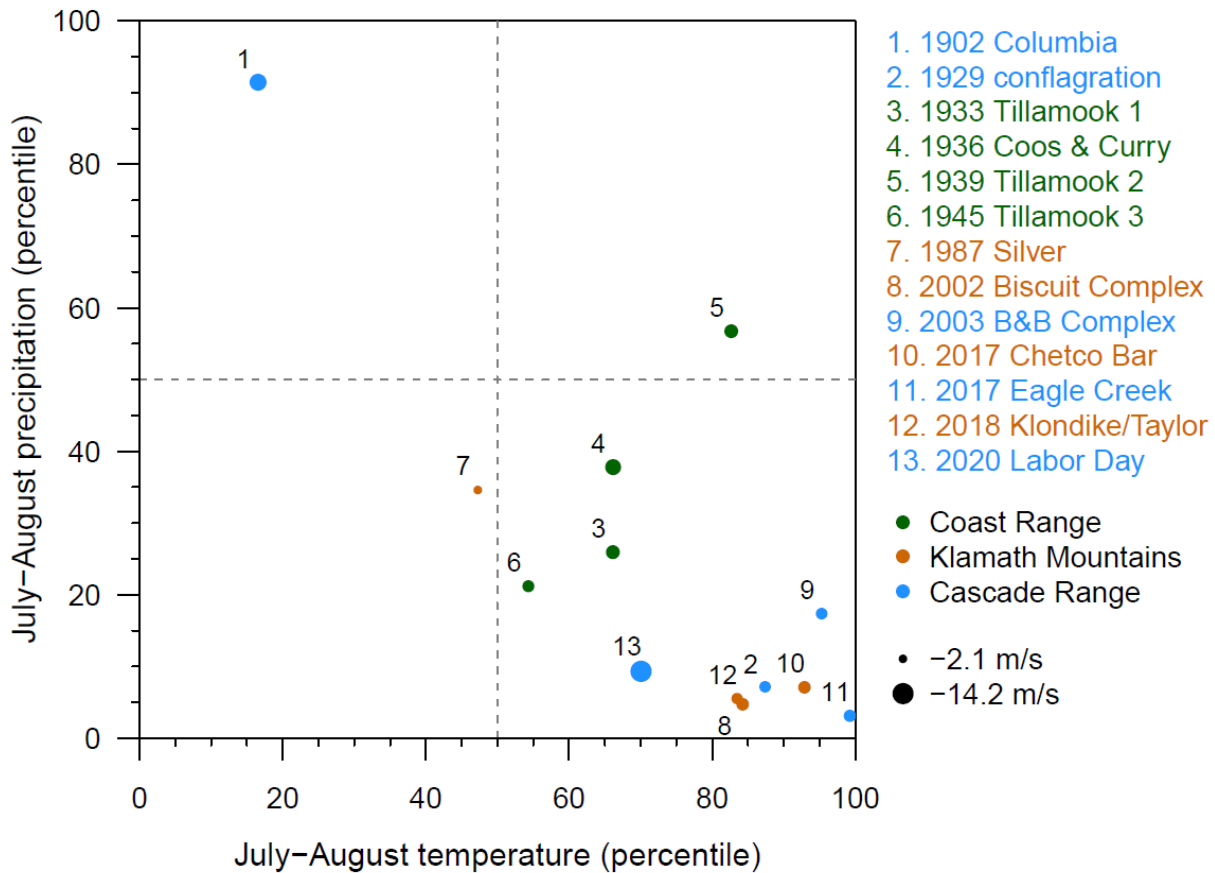


341
 342
 343
 344
 345
 346
 347
 348
 349
 350
 351
 352
 353
 354
 355

Figure 3: Scatter plots (a) wind speed and relative humidity (RH) at 1000hPa from the Salem, Oregon radiosonde for all July-September days during 1957-2020 at 0Z, and (b) daily maximum 6-hr easterly wind velocity at 700hPa/850hPa from NCEP-NCAR reanalyses and daily energy release component (ERC) averaged over the Oregon Cascades for all July-September days during 1979-2020. Negative easterly wind velocity refers to winds with a westerly component. Data in (b) are color-coded with daily burning index (BI) averaged over the Oregon Cascades. Points marked with black edge show data for 0Z 9 September 2020 (17 LST 8 September 2020) in (a) and 8 September 2020 in (b). Light-red shaded areas highlight the univariate space and events that exceed this point, while the dark-red shaded areas show the space that dominates this point in a bivariate AND-scenario case. Light grey horizontal and vertical lines show percentile values. Percentiles in both panels were computed relative to the entire July-September period of record. Percentiles are shown for wind speed in panel (b) rather than exclusively easterly wind velocity.



356
 357 **Figure 4:** Percentiles of (a) Energy Release Component (ERC), and (b) Burning Index (BI) for 8
 358 September 2020. Percentiles were tabulated based on data pooled over the entire calendar year
 359 1979-2020. Time series of (c) ERC and (d) BI aggregated over the Oregon Cascades for 2020
 360 (red), compared both the climatological 1981-2010 averages (black) and smoothed 5th to 95th
 361 percentile values (grey shading).
 362



363
 364 **Figure 5.** July-August total precipitation vs. July-August mean daily maximum temperature for
 365 the years of the large wildfires in western Oregon listed in Table S1. Values are given as
 366 percentiles of the anomalies for the years 1895 through 2020 (126 years). The percentiles shown
 367 for each event are calculated with respect to the anomalies for the county/counties where the
 368 event occurred. Symbols are sized relative to the peak easterly wind component at 700 or 850-
 369 hPa at 45°N, 122.5°W from 6-hourly NCEP-NCAR reanalysis (1948-present) and 20th Century
 370 reanalysis (1900-1947).
 371

372 Abatzoglou, J.T., & Kolden, C. A. (2013). Relationships between climate and macroscale area
373 burned in the western United States. *International Journal of Wildland Fire*, 22(7), 1003–
374 1020. <https://doi.org/10.1071/WF13019>

375 Abatzoglou, J.T., & Williams, A. P. (2016). Impact of anthropogenic climate change on wildfire
376 across western US forests. *Proceedings of the National Academy of Sciences*, 113(42),
377 11770–11775. <https://doi.org/10.1073/pnas.1607171113>

378 Abatzoglou, John T. (2013). Development of gridded surface meteorological data for ecological
379 applications and modelling. *International Journal of Climatology*, 33(1), 121–131.

380 Abatzoglou, John T, Hatchett, B. J., Fox-Hughes, P., Gershunov, A., & Nauslar, N. J. (2020). Global
381 climatology of synoptically-forced downslope winds. *International Journal of Climatology*.

382 Agee, J. K. (1996). *Fire ecology of Pacific Northwest forests*. Island press.

383 AghaKouchak, A., Cheng, L., Mazdiyasn, O., & Farahmand, A. (2014). Global warming and
384 changes in risk of concurrent climate extremes: Insights from the 2014 California drought.
385 *Geophysical Research Letters*, 41(24), 8847–8852.

386 Alizadeh, M. R., Adamowski, J., Nikoo, M. R., AghaKouchak, A., Dennison, P., & Sadegh, M.
387 (2020). A century of observations reveals increasing likelihood of continental-scale
388 compound dry-hot extremes. *Science Advances*, 6(39), eaaz4571.

389 Barbero, R., Abatzoglou, J. T., Steel, E. A., & Larkin, N. K. (2014). Modeling very large-fire
390 occurrences over the continental United States from weather and climate forcing.
391 *Environmental Research Letters*, 9(12), 124009. [https://doi.org/10.1088/1748-](https://doi.org/10.1088/1748-9326/9/12/124009)
392 [9326/9/12/124009](https://doi.org/10.1088/1748-9326/9/12/124009)

393 Beals, E. A. (1914). The value of weather forecasts in the problem of protecting forests from fire.
394 *Monthly Weather Review*, 42(2), 111–119.

395 Bowman, D. M. J. S., Balch, J. K., Artaxo, P., Bond, W. J., Carlson, J. M., Cochrane, M. A., et al.
396 (2009). Fire in the Earth system. *Science*, 324(5926), 481–484.

397 Bradstock, R. A. (2010). A biogeographic model of fire regimes in Australia: current and future
398 implications. *Global Ecology and Biogeography*, 19(2), 145–158.
399 <https://doi.org/10.1111/j.1466-8238.2009.00512.x>

400 Cohen, J. E., & Deeming, J. D. (1985). The National Fire-Danger Rating System: basic equations.
401 *Gen. Tech. Report*, 16.

402 Compo, G. P., Whitaker, J. S., Sardeshmukh, P. D., Matsui, N., Allan, R. J., Yin, X., et al. (2011). The
403 twentieth century reanalysis project. *Quarterly Journal of the Royal Meteorological Society*,
404 137(654), 1–28.

405 Cramer, O. P. (1957). *Frequency of dry east winds over northwest Oregon and southwest*
406 *Washington*. Pacific Northwest Forest and Range Experiment Station, Forest Service, US

407 Crimmins, M. A. (2006). Synoptic climatology of extreme fire-weather conditions across the
408 southwest United States. *International Journal of Climatology*, 26(8), 1001–1016.

409 Dague, C. I. (1930). Disastrous fire weather of September, 1929. *Monthly Weather Review*, 58,
410 368–370.

411 Dague, C. I. (1934). The weather of the great Tillamook, Oreg., Fire of August 1933. *Monthly*
412 *Weather Review*, 62, 227–231.

413 Daly, C., Halbleib, M., Smith, J. I., Gibson, W. P., Doggett, M. K., Taylor, G. H., et al. (2008).
414 Physiographically sensitive mapping of climatological temperature and precipitation across
415 the conterminous United States. *International Journal of Climatology*, 28(15), 2031–2064.

416 Durre, I., Vose, R. S., & Wuertz, D. B. (2006). Overview of the integrated global radiosonde
417 archive. *Journal of Climate*, 19(1), 53–68.

418 Goss, M., Swain, D., Abatzoglou, J., Sarhadi, A., Kolden, C., Williams, A., & Diffenbaugh, N. (2020).
419 Climate change is increasing the risk of extreme autumn wildfire conditions across
420 California. *Environmental Research Letters*.

421 Guzman-Morales, J., & Gershunov, A. (2019). Climate Change Suppresses Santa Ana Winds of
422 Southern California and Sharpens Their Seasonality. *Geophysical Research Letters*.

423 Guzman-Morales, J., Gershunov, A., Theiss, J., Li, H., & Cayan, D. (2016). Santa Ana Winds of
424 Southern California: Their climatology, extremes, and behavior spanning six and a half
425 decades. *Geophysical Research Letters*, 43(6), 2827–2834.

426 Hersbach, H., Bell, B., Berrisford, P., Hirahara, S., Horányi, A., Muñoz-Sabater, J., et al. (2020). The
427 ERA5 global reanalysis. *Quarterly Journal of the Royal Meteorological Society*, 146(730),
428 1999–2049.

429 Higuera, P. E., & Abatzoglou, J. T. (2020). Record-setting climate enabled the extraordinary 2020
430 fire season in the western United States. *Global Change Biology*, n/a(n/a).
431 <https://doi.org/10.1111/gcb.15388>

432 Horel, J., Splitt, M., Dunn, L., Pechmann, J., White, B., Ciliberti, C., et al. (2002). Mesowest:
433 Cooperative mesonets in the western United States. *Bulletin of the American
434 Meteorological Society*, 83(2), 211–226.

435 Hughes, M., Hall, A., & Kim, J. (2011). Human-induced changes in wind, temperature and relative
436 humidity during Santa Ana events. *Climatic Change*, 109(1), 119–132.

437 Jolly, W. M., Freeborn, P. H., Page, W. G., & Butler, B. W. (2019). Severe Fire Danger Index: A
438 Forecastable Metric to Inform Firefighter and Community Wildfire Risk Management. *Fire* .
439 <https://doi.org/10.3390/fire2030047>

440 Kallander, R. M. (1953). Problems of rehabilitating the Tillamook burn.

441 Khaykin, S., Legras, B., Bucci, S., Sellitto, P., Isaksen, L., Tencé, F., et al. (2020). The 2019/20
442 Australian wildfires generated a persistent smoke-charged vortex rising up to 35 km
443 altitude. *Communications Earth & Environment*, 1(1), 1–12.

444 Khorshidi, M. S., Dennison, P. E., Nikoo, M. R., AghaKouchak, A., Luce, C. H., & Sadegh, M. (2020).
445 Increasing concurrence of wildfire drivers tripled megafire critical danger days in Southern
446 California between 1982 and 2018. *Environmental Research Letters*, 15(10), 104002.

447 Kolden, C., & Abatzoglou, J. (2018). Spatial Distribution of Wildfires Ignited under Katabatic
448 versus Non-Katabatic Winds in Mediterranean Southern California USA. *Fire* .
449 <https://doi.org/10.3390/fire1020019>

450 Morris, W. G. (1934). Forest fires in western Oregon and western Washington. *Oregon Historical
451 Quarterly*, 35(4), 313–339.

452 Nauslar, N., Abatzoglou, J., & Marsh, P. (2018). The 2017 North Bay and Southern California
453 Fires: A Case Study. *Fire* . <https://doi.org/10.3390/fire1010018>

454 Plummer, F. G. (1912). *Forest fires: their causes, extent, and effects, with a summary of recorded
455 destruction and loss*. US Department of Agriculture, Forest Service.

456 Reilly, M. J., Dunn, C. J., Meigs, G. W., Spies, T. A., Kennedy, R. E., Bailey, J. D., & Briggs, K. (2017).
457 Contemporary patterns of fire extent and severity in forests of the Pacific Northwest, USA
458 (1985–2010). *Ecosphere*, 8(3), e01695.

459 Rothermel, R. C. (1972). *A mathematical model for predicting fire spread in wildland fuels* (Vol.

460 115). Intermountain Forest & Range Experiment Station, Forest Service, US ...
461 Rothermel, R. C. (1991). *Predicting behavior and size of crown fires in the Northern Rocky*
462 *Mountains* (Vol. 438). US Department of Agriculture, Forest Service, Intermountain Forest
463 and Range ...
464 Rupp, D. E., Li, S., Mote, P. W., Shell, K. M., Massey, N., Sparrow, S. N., Wallom, D. C. H., & Allen,
465 M. R. (2017). Seasonal spatial patterns of projected anthropogenic warming in complex
466 terrain: a modeling study of the western US. *Climate Dynamics*, 48(7-8), 2191-2213.
467 doi:10.1007/s00382-016-3200-x
468 Sadegh, M., Moftakhari, H., Gupta, H. V., Ragno, E., Mazdiyasn, O., Sanders, B., et al. (2018).
469 Multihazard scenarios for analysis of compound extreme events. *Geophysical Research*
470 *Letters*, 45(11), 5470–5480.
471 Salvadori, G., Durante, F., De Michele, C., Bernardi, M., & Petrella, L. (2016). A multivariate
472 copula-based framework for dealing with hazard scenarios and failure probabilities. *Water*
473 *Resources Research*, 52(5), 3701–3721.
474 Seneviratne, S., Nicholls, N., Easterling, D., Goodess, C., Kanae, S., Kossin, J., et al. (2012).
475 Changes in climate extremes and their impacts on the natural physical environment.
476 Sharples, J. J., Mills, G. A., McRae, R. H. D., & Weber, R. O. (2010). Foehn-like winds and elevated
477 fire danger conditions in southeastern Australia. *Journal of Applied Meteorology and*
478 *Climatology*, 49(6), 1067–1095.
479 State of Oregon. Retrieved February 23, 2021, from
480 [https://www.oregon.gov/gov/policy/Documents/WERC-](https://www.oregon.gov/gov/policy/Documents/WERC-2020/Wildfire%20Report%20FINAL.pdf)
481 [2020/Wildfire%20Report%20FINAL.pdf](https://www.oregon.gov/gov/policy/Documents/WERC-2020/Wildfire%20Report%20FINAL.pdf)
482 Tedim, F., Leone, V., Amraoui, M., Bouillon, C., Coughlan, R. M., Delogu, M. G., et al. (2018).
483 Defining Extreme Wildfire Events: Difficulties, Challenges, and Impacts. *Fire* .
484 <https://doi.org/10.3390/fire1010009>
485 Williams, A. P., Abatzoglou, J. T., Gershunov, A., Guzman-Morales, J., Bishop, D. A., Balch, J. K., &
486 Lettenmaier, D. P. (2019). Observed impacts of anthropogenic climate change on wildfire in
487 California. *Earth's Future*, 7, 892–910.
488 Wohland, J., Omrani, N.-E., Witthaut, D., & Keenlyside, N. S. (2019). Inconsistent Wind Speed
489 Trends in Current Twentieth Century Reanalyses. *Journal of Geophysical Research:*
490 *Atmospheres*, 124(4), 1931–1940. <https://doi.org/https://doi.org/10.1029/2018JD030083>
491